

# Pulse plated $\text{CdS}_x\text{Te}_{1-x}$ films and their properties

K.R. Murali<sup>a,\*</sup>, P. Thirumoorthy<sup>b</sup>, C. Kannan<sup>d</sup>, V. Sengodan<sup>c</sup>

<sup>a</sup> *Electrochemical Materials Science Division, Central Electrochemical Research Institute, Karaikudi 630 006, India*

<sup>b</sup> *Department of Electronics, KSR College of Arts and Science, Tiruchengode, India*

<sup>c</sup> *Department of Electronics, SNR Sons College, Coimbatore, India*

<sup>d</sup> *Department of Physics, KSR College of Engineering and Technology, Tiruchengode, India*

Received 3 February 2008; received in revised form 19 June 2008; accepted 19 June 2008

Available online 22 July 2008

Communicated by: Associate Editor T.M. Razykov

## Abstract

$\text{CdS}_x\text{Te}_{1-x}$  films were deposited on titanium and conducting glass substrates at room temperature using 0.25 M cadmium sulphate, the concentration of sodium thiosulphate and  $\text{TeO}_2$  dissolved in sodium hydroxide was varied in the range of 0.01–0.05 M. The as deposited films exhibited hexagonal structure irrespective of the composition. The FWHM maximum of the x-ray diffraction peaks were found to decrease with increase of duty cycle. The optical energy gap values are in the range of 1.54–2.32 eV for films of different composition, it is observed that the band gap shifts towards CdS side as the concentration of CdS in the films increase. XPS studies indicated the formation of CdSTe solid solution. The grain size increases from 11.54 to 99.40 nm as the value of  $x$  increases from 0.2 to 0.8. The surface roughness is found to increase from 0.22 to 2.50 nm as the value of ' $x$ ' increases from 0.2 to 0.8. The resistivity is found to vary from 53 to 8 ohm cm as the ' $x$ ' value decreases from 1 to 0.

© 2008 Elsevier Ltd. All rights reserved.

**Keywords:** Thin films; Semiconductors; Brush plating; Electrodeposition

## 1. Introduction

Thin film photovoltaic solar cells based on n-type CdS window layers and p-type CdTe absorber layers have been extensively studied for many years (Romeo et al., 2004; Compaan et al., 2004), and the formation of an intermediate layer of  $\text{CdS}_x\text{Te}_{1-x}$  during cell fabrication is now widely acknowledged. This layer results from inter-diffusion and is believed to affect device efficiency through the resulting change in the optical band gap. Thin films of  $\text{CdS}_x\text{Te}_{1-x}$  have been earlier deposited by chemical bath deposition (Patil et al., 2001, 2004), pulsed laser deposition (Wood et al., 2000), vacuum evaporation (Rogers et al., 1999; Al-Ani et al., 1993), electron beam evaporation (Hill and Richardson, 1973) and slurry coating (Santana-

Aranda and Meléndez-Lira, 2001). This is the first report on pulse electrodeposited  $\text{CdS}_x\text{Te}_{1-x}$  films. In this paper, the results obtained on the pulse plated  $\text{CdS}_x\text{Te}_{1-x}$  films are presented and discussed.

## 2. Experimental methods

$\text{CdS}_x\text{Te}_{1-x}$  films were deposited on titanium and conducting glass substrates of size 2 cm long and 1 cm wide, at room temperature using 0.25 M cadmium sulphate, the concentration of sodium thiosulphate and  $\text{TeO}_2$  dissolved in sodium hydroxide was varied in the range of 0.01–0.05 M. As an example, for the deposition of  $\text{CdS}_{0.5}\text{Te}_{0.5}$  film, the precursors were taken with the following concentration, 20 ml of 0.25 M  $\text{CdSO}_4$ , 1 ml of 0.025 M  $\text{TeO}_2$  and 1 ml of 0.025 M sodium thiosulphate. All chemicals were of Analar grade purity. The pH of the bath was adjusted to 2.0 by adding sulphuric acid. The deposition potential

\* Corresponding author. Tel.: +91 4565 227550; fax: +91 4565 227553.  
E-mail address: [muraliramkrish@gmail.com](mailto:muraliramkrish@gmail.com) (K.R. Murali).

was maintained at  $-0.80$  V (SCE). The conducting glass and titanium substrates were cleaned prior to deposition. The duty cycle was varied in the range of 6–50%. The deposition time was 60 min in all the cases. Thickness of the films estimated by Mitutoyo surface profilometer was  $2.0$   $\mu\text{m}$ . Uniformity of the deposit was found by measuring the resistivity profile across the deposit and it was observed that the resistivity varied within 0.3%. The films were characterized by X-ray diffraction using a PANalytical X-ray diffractometer. Optical absorption measurements were made on the films deposited on conducting glass substrates using Hitachi U3400 UV–VIS–NIR spectrophotometer. Surface morphology studies were made using Molecular Imaging Systems Atomic force microscope. EDAX measurements were made on the films using a JEOL SEM fitted with EDAX attachment. XPS studies were made using MK III VG ESCA system.

Generally in electrodeposition technique for producing a metal or compound, a driving force (i.e., the free energy) in the form of a potential or current is applied to the electrode. Either of these can be used as a variable as in the case of continuous electrodeposition. But modern electronics allow one to make use of these parameters as a function of time. This permits a number of possible ways of varying the conditions.

Four variable parameters are of primary importance in pulse plating. They are

- (1) Peak current density,  $i_p$
- (2) Average current density,  $i_a$
- (3) ON time,
- (4) OFF time.

The sum of the ON and OFF times constitute one pulse cycle. The duty cycle is defined as follows:

$$\text{Duty cycle} = \frac{\text{ON time}}{\text{ON time} + \text{OFF time}} \times 100\% \quad (1)$$

A duty cycle of 100% corresponds to conventional plating because OFF time is zero.

In practice, pulse plating usually involves a duty cycle of 5% or greater. The average current density ( $i_a$ ) under pulse plating conditions is defined as

$$\begin{aligned} i_a &= \text{peak current density} \times \text{duty cycle} \\ &= i_p \times \text{duty cycle} \end{aligned} \quad (2)$$

During the ON time the concentration of the metal ions to be deposited is reduced within a certain distance from the cathode surface. This so-called diffusion layer pulsates with the same frequency as the applied pulse current. Its thickness is also related to  $i_p$  but reaches a limiting value governed primarily by the diffusion coefficient of the metal ions. During the OFF time the concentration of the metal

ions build up again by diffusion from the bulk electrolyte and will reach the equilibrium concentration of the bulk electrolyte if enough time is allowed.

These variables result in two important characteristic features of pulse plating which make it useful for alloy plating as well as property changes as mentioned earlier. They are

- (i) Very high instantaneous current densities and hence very high negative potentials can be reached. The high over potential causes a shift in the ratio of the rates of reactions with different kinetics. This high over potential associated with the high pulse current density greatly influences the nucleation rate because a high energy is available for the formation of new nuclei.
- (ii) The second characteristics feature is the influence of the OFF time during which important adsorption and desorption phenomena as well as recrystallization of the deposit occur.

### 3. Results and discussion

The as deposited films exhibited hexagonal structure irrespective of the composition. Results on pulsed laser deposited CdSTe films indicated that the films deposited below  $x = 0.5$  in  $\text{CdS}_x\text{Te}_{1-x}$  films exhibited cubic structure, whereas films deposited at values greater  $x = 0.5$  exhibited hexagonal structure (Hill and Richardson, 1973). For screen printed  $\text{CdS}_x\text{Te}_{1-x}$  films, films exhibited cubic structure for  $x < 0.3$  and hexagonal structure for higher values of  $x$  (Santana-Aranda and Meléndez-Lira, 2001). In this study only single phase hexagonal structure was observed for all compositions. The FWHM (Fullwidth at half maximum) of the XRD peaks were found to decrease with increase of duty cycle. Fig. 1 shows the XRD pattern of the  $\text{CdS}_{0.5}\text{Te}_{0.5}$  films deposited at different duty cycles. Peaks corresponding to CdS or CdTe were absent. The peaks were observed to shift towards low  $2\theta$  side as the concentration of CdTe increased in the ternary. The intensity of the peaks increased with increase of duty cycle. This may be attributed to the fact that as the duty cycle increases, the thickness of the films increase, hence the intensity of the peaks increase. The peaks corresponding to the (100), (002), (101), (102), (110) and (112) reflection were observed in all the cases. The peaks were found to shift from CdTe to CdS side as the concentration of CdS increased in the films. Fig. 2 shows the variation of lattice spacing of CdS with increase of CdTe concentration. The lattice parameters were evaluated using the equation

$$1/d^2 = 4/3a^2(h^2 + k^2 + l^2) + l/c^2$$

Fig. 3 shows the variation of lattice parameters ' $a$ ' and ' $c$ ' with composition. The variation is linear and obeys Vegard's law. The lattice parameters changed from CdTe to CdS side as the concentration of CdS increased in the

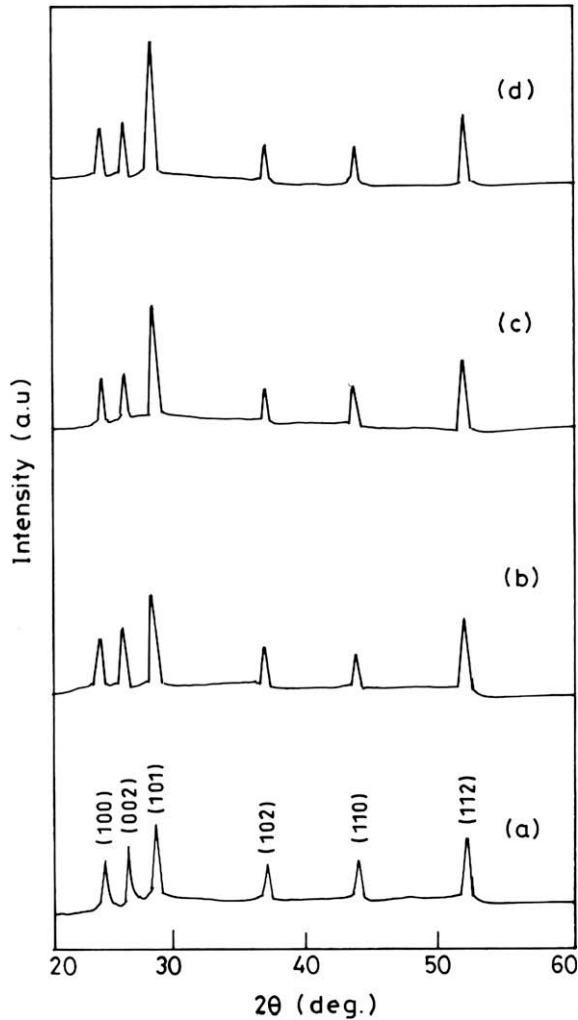


Fig. 1. X-ray diffraction pattern of the CdS<sub>0.5</sub>Te<sub>0.5</sub> films deposited at different duty cycles: (a) 10%; (b) 15%; (c) 33%; (d) 50%.

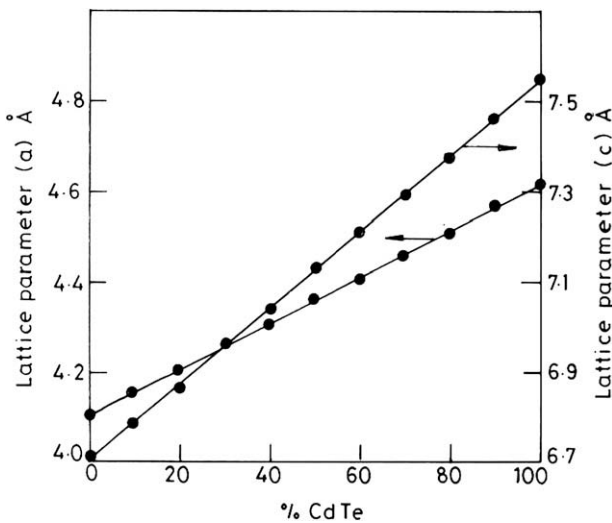


Fig. 2. Variation of lattice spacing of CdS<sub>x</sub>Te<sub>1-x</sub> with increase of CdTe concentration.

films. Large crystallites produce sharp peaks, while, very tiny crystallites produce broad XRD peaks. Small crystal-

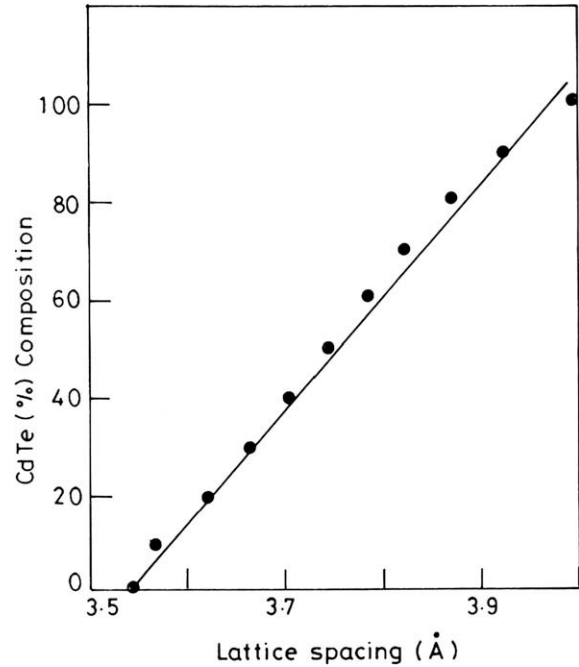


Fig. 3. Variation of lattice parameters 'a' and 'c' with composition.

lites allow X-ray beam to diverge as it leaves since the diffraction peaks are no longer infinite in length as compared to the incident wavelength. Thus, these crystallites do not collimate the X-ray beam as effectively as large crystallites and hence produce a broad diffraction peak.

Optical absorption studies were made on the films of different composition deposited at a duty cycle of 50% on conducting glass substrates. Plots of  $(\alpha hv)^2$  vs  $hv$  are shown in Figs. 4 and 5. The plots were linear suggesting direct band nature of the films. The extrapolated values of the optical energy gap,  $E_g$ , are in the range of 1.54–2.32 eV for films of different composition, it is observed that the band gap shifts towards CdS side as the concentration of CdS in the films increase Fig. 6 shows the variation of band gap with CdTe percentage. The band gap was found to

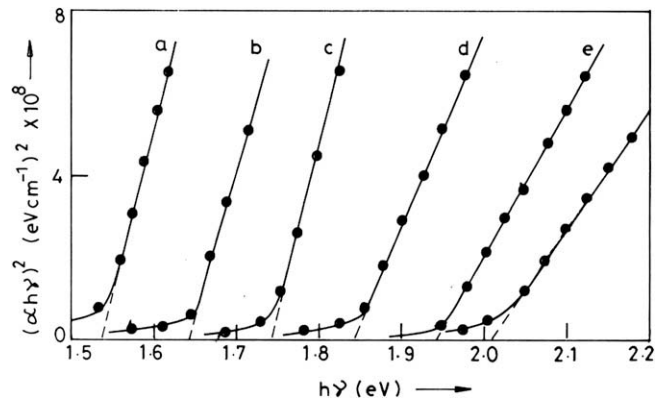


Fig. 4.  $(\alpha hv)^2$  vs  $h\nu$  plot of CdS<sub>x</sub>Te<sub>1-x</sub> films of different composition deposited at 50% duty cycle: (a)  $x = 0.1$ ; (b)  $x = 0.2$ ; (c)  $x = 0.3$ ; (d)  $x = 0.4$ ; (e)  $x = 0.5$ ; (f)  $x = 0.6$ .

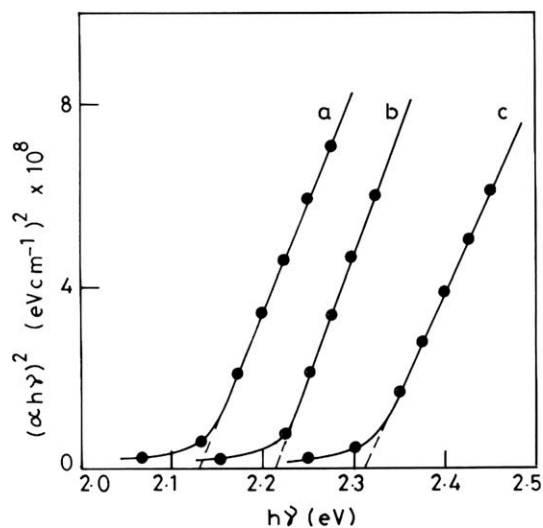


Fig. 5.  $(\alpha h\nu)^2$  vs  $h\nu$  plot of  $\text{CdS}_x\text{Te}_{1-x}$  films of different composition deposited at 50% duty cycle: (a)  $x = 0.7$ ; (b)  $x = 0.8$ ; (c)  $x = 0.9$ .

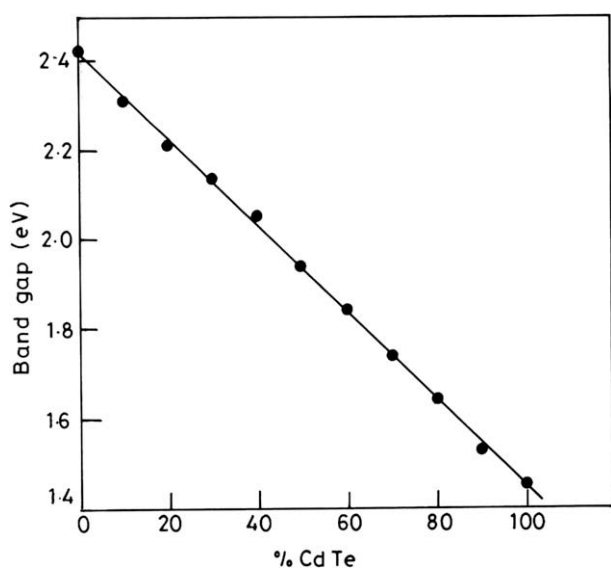


Fig. 6. Variation of band gap with CdTe percentage.

vary from 1.44 to 2.41 eV as the percentage of CdS increased. Similar results were observed for chemically deposited films, screen printed films and pulse laser deposited films (Gordillo and Romero, 2005; Santana-Aranda et al., 2001; Patil et al., 2001).

EDAX measurements were made on the films of different composition heat treated at 550 °C and the EDAX spectrum of the films deposited with equal concentration of S and Te precursors is shown in Fig. 7. Peaks corresponding to  $\text{CdL}\alpha_1$ ,  $\text{TeL}\alpha$ , S  $\text{K}\alpha$  were observed in the EDAX spectrum. From Fig. 7 the composition is Cd – 51%, S – 24%, Te – 25%. In all the compositions, a slight excess of Cd was observed.

XPS spectrum was taken for the films of different composition. The  $\text{Cd}3d_{5/2}$  and  $\text{Cd}3d_{3/2}$  appeared in the range

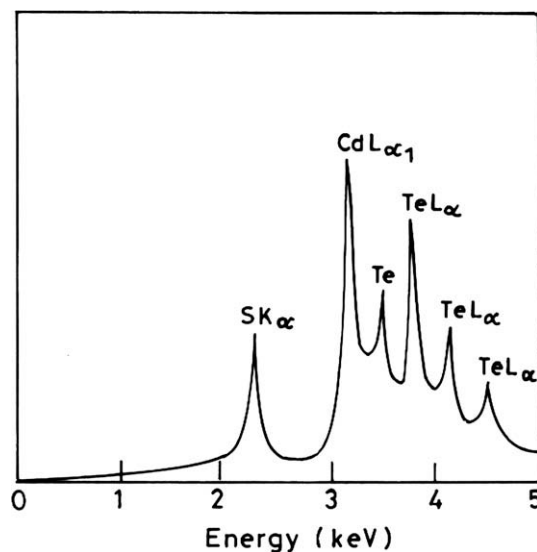


Fig. 7. EDAX spectrum of  $\text{CdS}_{0.5}\text{Te}_{0.5}$  films deposited at 50% duty cycle.

405.7–409 eV and 412.5–414.5 eV, respectively, the  $\text{Te}3d_{5/2}$  and  $\text{Te}3d_{3/2}$  appeared in the range 568–574 eV and 578–584 eV, respectively, and the  $\text{S}3d_{5/2}$  and  $\text{S}3d_{3/2}$  appeared in the range 157–161 eV and 163–167 eV, respectively, as the  $x$  value changes from 0 to 1. Fig. 8 shows the XPS spectrum of the  $\text{CdS}_{0.5}\text{Te}_{0.5}$  film as a representative. The values of binding energies for Cd and S in CdS films correspond to the  $\text{Cd}3d_{5/2}$  and  $\text{Cd}3d_{3/2}$  appearing at 405 and 411.7 eV and to the S ( $3d_{5/2}$  and  $3d_{3/2}$ ) levels at 168.0 eV and 173.0 eV. The value of the binding energy obtained for  $\text{Cd}3d_{5/2}$  and  $\text{Cd}3d_{3/2}$  is similar to values of Cd in CdS reported earlier (Luan et al., 2006). The values of binding energies for Cd and Te in CdTe films correspond to the  $\text{Cd}3d_{5/2}$  and  $\text{Cd}3d_{3/2}$  appearing at 412.5 eV and 420.7 eV and to the Te ( $3d_{5/2}$  and  $3d_{3/2}$ ) levels at 580 eV and 583 eV (Chen et al., 1997). The splitting seen in Te 3d peak is due to the presence of Te–Cd bonding in CdTe (Chen et al., 1997). The Te peaks did not split further into a high energy component corresponding to Te–O bonds, hence oxides are not present. The values of the binding energy are observed to shift from CdTe side to CdS side as the concentration of CdS in the films increases.

Atomic force micrographs were taken on the films of different composition deposited at a duty cycle of 50%. Fig. 9 shows the atomic force micrographs of  $\text{CdS}_x\text{Te}_{1-x}$  films of different composition deposited at 50% duty cycle. It is observed from the figures, that the grain size increases from 11.54 to 99.40 nm as the value of  $x$  increases from 0.2 to 0.8. The surface roughness is found to increase from 0.22 to 2.50 nm as the value of ‘ $x$ ’ increases from 0.2 to 0.8. The values of surface roughness as well as the grain size reported above have been obtained as a print output from the Atomic force microscope.

The conduction mechanism in semiconductors can be understood by analyzing current voltage plots ( $I$ – $V$  plots). For single carrier injection at low voltages, the plot is gen-

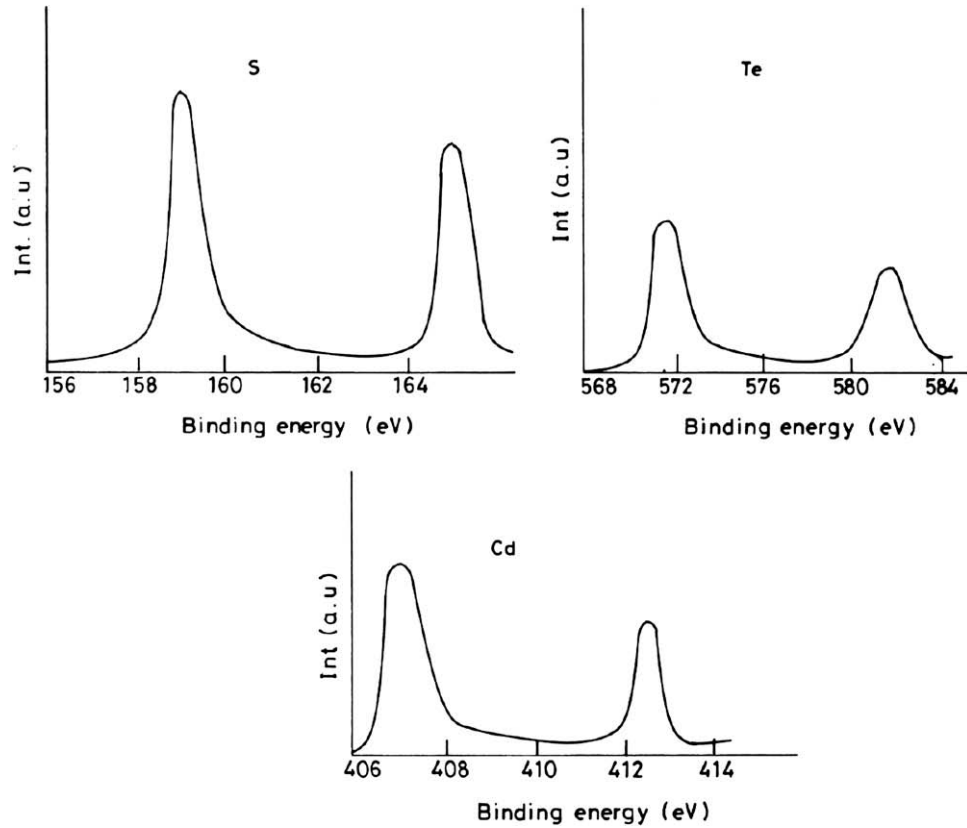


Fig. 8. XPS spectrum of the  $\text{CdS}_{0.5}\text{Te}_{0.5}$  film deposited at 50% duty cycle.

erally a straight line, showing the validity of Ohm's law. However, at higher voltages, some deviation is expected.  $I$ - $V$  characteristics of films deposited at 50% duty cycle and of different composition were measured by providing Indium dot contact at the centre of the top surface and is shown in Fig. 10. The plots are linear. Resistivity of the films was calculated from the slope of the plots. The resistivity is found to vary from 53 ohm cm to 8 ohm cm as the 'x' value decreases from 1 to 0. The resistivity values are shown in Table 1. The resistivity of the films obtained in this study is lower than that obtained by chemical bath deposited films (Patil et al., 2001, 2004). To cross check the resistivity data, the films deposited on conducting glass substrates were transferred on to an epoxy resin following the procedure given in Miyake et al. (2004). In this method, the  $\text{CdS}_x\text{Te}_{1-x}$  films are mechanically transferred from the conducting substrate onto a non-conductive epoxy resin without the formation of cracks (Miyake et al., 2003; Von Windheim et al., 1991). The electrical resistivity measurements were made using Van der Pauw method after providing Indium ohmic contacts on the top surface of the films. The resistivity values obtained by the above method vary from 55 to 10 ohm cm. The low resistivity observed in these films is due to the slight excess of cadmium as observed from EDAX measurements. Hot probe measurements indicated the films to exhibit n-type behavior.

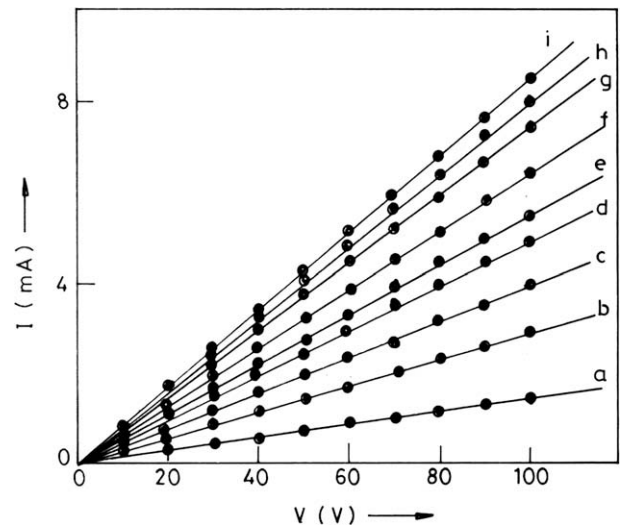


Fig. 9. Atomic force micrographs of  $\text{CdS}_x\text{Te}_{1-x}$  films of different composition deposited at 50% duty cycle: (a)  $x = 0.2$ ; (b)  $x = 0.4$ ; (c)  $x = 0.8$ .

Preliminary studies on the photoelectrochemical cells using the as deposited films, indicated an open circuit voltage value of 0.40 V and a short circuit current density of  $2.0 \text{ mA cm}^{-2}$ . These values are higher than the values reported on chemical bath deposited films (Patil et al., 1997).

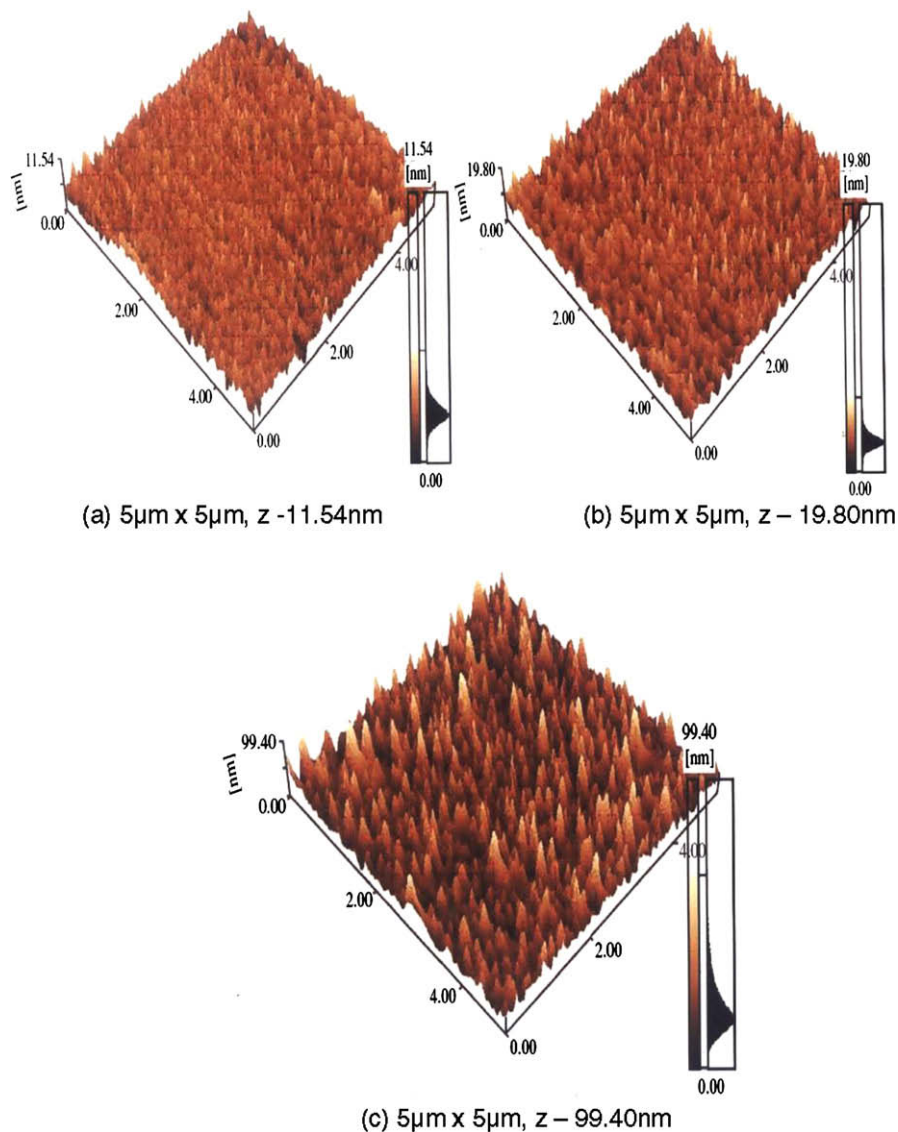


Fig. 10.  $I-V$  Characteristics of  $\text{CdS}_x\text{Te}_{1-x}$  films deposited at 50% duty cycle and of different composition: (a)  $x = 0.9$ ; (b)  $x = 0.8$ ; (c)  $x = 0.7$ ; (d)  $x = 0.6$ ; (e)  $x = 0.5$ ; (f)  $x = 0.4$ ; (g)  $x = 0.3$ ; (h)  $x = 0.2$ ; (i)  $x = 0.1$ .

Table 1  
Variation of Resistivity with composition of  $\text{CdS}_x\text{Te}_{1-x}$  films deposited at 50% duty cycle

Composition ( $x$ )	Resistivity (ohm cm)
0.1	8.0
0.2	9.2
0.3	9.7
0.4	12.2
0.5	16.7
0.6	20.0
0.7	29.0
0.8	35.8
0.9	53.0

#### 4. Conclusion

The results of this study clearly indicate that  $\text{CdS}_x\text{Te}_{1-x}$  films with resistivity in the range of 53–8 ohm cm can

be easily obtained by this technique. Nanocrystalline films with crystallite size in the range of 11–100 nm can be easily obtained by this technique. Large area electrodes can be deposited and further work is in progress in this direction.

#### References

- Al-Ani, S.K.J., Makadsi, M.N., Al-Shakarchi, I.K., Hogarth, C.A., 1993. *J. Mater. Sci.* 28, 251.
- Chen, K.T., Shi, D.T., Chen, H., Granderson, B., George, M.A., Collins, W.E., Burger, A., James, R.B., 1997. *J. Vac. Sci. Technol.* A15, 850.
- Compaan, A.D., Gupta, A., Lee, S., Wang, S., Drayton, J., 2004. *Sol. Energy* 77, 815.
- Gordillo, G., Romero, E., 2005. *Thin solid films* 484, 252.
- Hill, R., Richardson, D., 1973. *Thin Solid Films* 18, 25.
- Luan, Y., An, M., Lu, G., 2006. *Appl. Surf. Sci.* 253, 459.
- Miyake, M., Murase, K., Hirato, T., Awakura, Y., 2003. *J. Electrochem. Soc.* 150, C413.

- Miyake, M., Murase, K., Hirato, T., Awakura, Y., 2004. *J. Electroanal. Chem* 562, 247.
- Patil, V.B., Sutrave, S., Shahane, G.S., Deshmukh, L.P., 1997. *Int. J. Electron.* 83, 341.
- Patil, V.B., Sutrave, D.S., Shahane, G.S., Deshmukh, L.P., 2001. *Indian J. Pure Appl. Phys.* 39, 184.
- Patil, V.B., Sutrave, D., Shahane, G.S., Deshmukh, L.P., 2001. *Indian J. Pure Appl. Phys.* 39, 184.
- Patil, V.B., Shahane, G.S., Sutrave, D.S., Raut, B.T., Deshmukh, L.P., 2004. *Thin Solid Films* 446, 1.
- Rogers, K.D., Painter, J.D., Healy, M.J., Lane, D.W., Ozsar, M.E., 1999. *Thin solid Films* 339, 299.
- Romeo, N., Bosio, A., Canevari, V., Podestà, A., 2004. *Sol. Energy* 77, 795.
- Santana-Aranda, M.A., Meléndez-Lira, M., 2001. *Appl. Surf. Sci.* 175–176, 538.
- Santana-Aranda, M.A., Lira, M.M., 2001. *Appl. Surf. Sci.* 175–176, 538.
- Von Windheim, J.A., Wynands, H., Cocivera, M., 1991. *J. Electrochem. Soc.* 138, 3435.
- Wood, D.A., Rogers, K.D., Lane, D.W., Coath, J.A., 2000. *J. Phys. C: Condens. Matter* 12, 4433.